

KLOE searches on dark forces

S. GIOVANNELLA for the KLOE-2 COLLABORATION

INFN, Laboratori Nazionali di Frascati - via Enrico Fermi 40, Frascati, Italy

ricevuto il 7 Settembre 2012

Summary. — The existence of a secluded gauge sector could explain at the same time several unexpected astrophysical observations. This hypothesis can be tested at low energy e^+e^- colliders by searching for a light vector gauge boson, called U , mediating dark forces. At DAΦNE, the Frascati e^+e^- ϕ -factory, three different U boson production channels can be studied. Results obtained with KLOE data and perspectives for the KLOE-2 run, where a larger data sample is expected, are discussed.

PACS 14.70.Pw – Other gauge bosons.

1. – Dark matter and dark forces

Several recent astrophysical observations produced unexpected results, as the 511 keV gamma-ray signal from the galactic center observed by the INTEGRAL satellite [1], the excess in the cosmic ray positrons reported by PAMELA [2], the total electron and positron flux measured by ATIC [3], Fermi [4] and HESS [5, 6], the annual modulation of the DAMA/LIBRA signal [7, 8] and the low energy spectrum of nuclear recoil candidate events observed by CoGeNT [9]. These anomalies could be all explained with the existence of a dark matter weakly interacting massive particle, belonging to a secluded gauge sector under which the Standard Model (SM) particles are uncharged [10-19]. An abelian gauge field, the U boson with mass near the GeV scale, couples the secluded sector to the SM through its kinetic mixing with the SM hyper-charge gauge field. The kinetic mixing parameter, ϵ , is expected to be of the order 10^{-4} – 10^{-2} [11, 21], so that observable effects can be induced in $\mathcal{O}(\text{GeV})$ -energy e^+e^- colliders [20-24] and fixed target experiments [25-28]. The possible existence of a new light boson gauging a new symmetry with a small coupling was in fact already introduced on general grounds in [29], and rediscussed in models postulating also the existence of light spin 0 or 1/2 dark matter particles [30, 31]. This boson can have both vector and axial-vector couplings to quark and leptons, however axial couplings are strongly constrained by data, leaving room to vector couplings only.

2. – Searches for dark forces at KLOE

The KLOE experiment operates at DAΦNE, the e^+e^- Frascati ϕ -factory. From 2000 to 2006, KLOE collected 2.5 fb^{-1} of collisions at the ϕ meson peak and about 240 pb^{-1} below the ϕ resonance ($\sqrt{s} = 1 \text{ GeV}$). The ϕ meson predominantly decays into charged and neutral kaons, thus allowing KLOE to make precision studies in the fields of flavor physics, low-energy QCD and test of discrete symmetries [32].

A new beam crossing scheme allowing a reduced beam size and increased luminosity is operating at DAΦNE [33]. The KLOE-2 detector was successfully installed in this new interaction region and has been upgraded with small angle tagging devices to detect both high- and low-energy electrons or positrons in $e^+e^- \rightarrow e^+e^-X$ events. An inner tracker and small angle calorimeters are scheduled to be installed in a subsequent step, providing larger acceptance both for charged particles and photons. A detailed description of the KLOE-2 physics program can be found in ref. [34].

The U boson can be produced at DAΦNE through radiative decays of neutral mesons, such as $\phi \rightarrow \eta U$. With the statistics already collected at KLOE, this decay can potentially probe couplings down to $\epsilon \sim 10^{-3}$ [22], covering most of the parameter's range of interest for the theory. The U boson can be observed by its decay into a lepton pair, while the η can be tagged by one of its not-rare decays.

Assuming also the existence of a secluded Higgs boson, the h' , both the U and the h' can be produced at DAΦNE if their masses are smaller than M_ϕ . The mass of the U and h' are both free parameters, and the possible decay channels can be very different depending on which particle is heavier. In both cases, an interesting production channel is the h' -strahlung, $e^+e^- \rightarrow U h'$ [20]. Assuming the h' to be lighter than the U boson, it turns out to be very long-lived, so that the signature process will be a lepton pair, generated by the U boson decay, plus missing energy. In the case $m_{h'} > m_U$, the dark Higgs frequently decays to a pair of real or virtual U 's. In this case one can observe events with 6 leptons in the final state, due to the h' -strahlung process, or 4 leptons and a photon, due to the $e^+e^- \rightarrow h'\gamma$ reaction.

Another possible channel to look for the existence of the U boson is the $e^+e^- \rightarrow U\gamma$ process [20]. The expected cross-section can be as high as $\mathcal{O}(\text{pb})$ at DAΦNE energies. The on-shell boson can decay into a lepton pair, giving rise to a $\ell^+\ell^-\gamma$ signal of few MeV mass resolution. About $10^3 \text{ events/fb}^{-1}$ are expected to be produced for $\epsilon \sim 10^{-3}$.

In the following sections, results from the analyses of $\phi \rightarrow \eta U$ and $e^+e^- \rightarrow U h'$ channels are reported, together with perspectives for the new KLOE-2 run.

3. – The $\phi \rightarrow \eta U$ decay

As discussed above, the search of the U boson can be performed at KLOE using the decay chain $\phi \rightarrow \eta U$, $U \rightarrow \ell^+\ell^-$. An irreducible background due to the Dalitz decay of the ϕ meson, $\phi \rightarrow \eta \ell^+\ell^-$, is present. This decay has been studied by the SND and CMD-2 experiments, which measured a branching fraction of $\text{BR}(\phi \rightarrow \eta e^+e^-) = (1.19 \pm 0.19 \pm 0.07) \times 10^{-4}$ and $\text{BR}(\phi \rightarrow \eta e^+e^-) = (1.14 \pm 0.10 \pm 0.06) \times 10^{-4}$, respectively [35,36]. This corresponds to a cross-section of $\sigma(\phi \rightarrow \eta \ell^+\ell^-) \sim 0.7 \text{ nb}$, with a di-lepton mass range $M_{\ell\ell} < 470 \text{ MeV}$. For the signal, the expected cross-section is expressed by [22]

$$(1) \quad \sigma(\phi \rightarrow \eta U) = \epsilon^2 |F_{\phi\eta}(m_U^2)|^2 \frac{\lambda^{3/2}(m_\phi^2, m_\eta^2, m_U^2)}{\lambda^{3/2}(m_\phi^2, m_\eta^2, 0)} \sigma(\phi \rightarrow \eta\gamma),$$

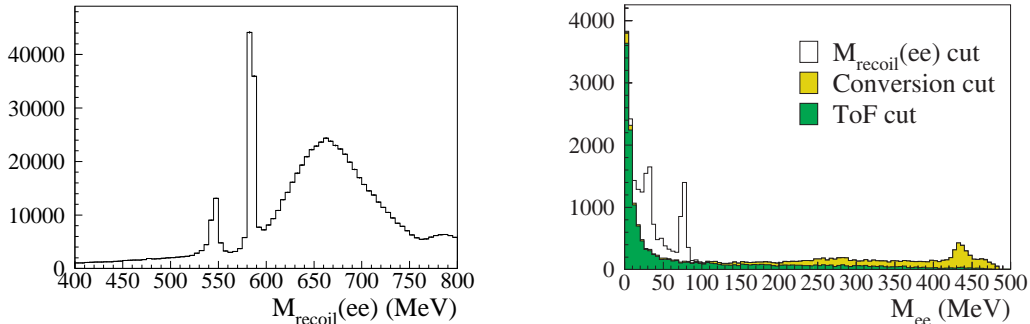


Fig. 1. – Left: Recoiling mass against the e^+e^- pair for data sample after preselection cuts. The $\phi \rightarrow \eta e^+e^-$ signal is clearly visible in the peak corresponding to η mass. The second peak at ~ 590 MeV is due to $K_S \rightarrow \pi^+\pi^-$ events with wrong mass assignment. Right: M_{ee} distribution for data at different analysis steps.

where $F_{\phi\eta}(m_U^2)$ is the $\phi\eta\gamma^*$ transition form factor evaluated at the U mass while the following term represents the ratio of the kinematic functions of the involved decays, with $\lambda(m_1^2, m_2^2, m_3^2) = [1 + m_3^2/(m_1^2 - m_2^2)]^2 - 4m_1^2m_3^2/(m_1^2 - m_2^2)^2$. Using $\epsilon = 10^{-3}$ and $|F_{\phi\eta}(m_U^2)|^2 = 1$, a cross-section $\sigma(\phi \rightarrow \eta U) \sim 40$ fb is obtained. Despite the small ratio between the overall cross-section of $\phi \rightarrow \eta U$ and $\phi \rightarrow \eta\ell^+\ell^-$, their different di-lepton invariant mass distributions allow to test the ϵ parameter down to 10^{-3} with the KLOE data set.

The best U decay channel to search for the $\phi \rightarrow \eta U$ process at KLOE is in e^+e^- , since a wider range of U boson masses can be tested and e^\pm are easily identified using a time-of-flight (ToF) technique. The η can be tagged by the three-pion or two-photon final state, which represent $\sim 95\%$ of the total decay rate. We have performed a search using the $\eta \rightarrow \pi^+\pi^-\pi^0$ channel, which provide a clean signal with four charged tracks and two photon in the final state. Studies are under way also for the $\eta \rightarrow \pi^0\pi^0\pi^0$ and $\eta \rightarrow \gamma\gamma$ samples.

3.1. The $\eta \rightarrow \pi^+\pi^-\pi^0$ final state. – The analysis of the $\eta \rightarrow \pi^+\pi^-\pi^0$ final state has been performed on 1.5fb^{-1} . The Monte Carlo (MC) simulation of the irreducible background $\phi \rightarrow \eta e^+e^-$, $\eta \rightarrow \pi^+\pi^-\pi^0$ has been produced with $d\Gamma(\phi \rightarrow \eta e^+e^-)/dm_{ee}$ weighted according to Vector Meson Dominance model [37], using the form factor parametrization from the SND experiment [35]. The MC simulation for the $\phi \rightarrow \eta U$ decay has been developed according to [22], with a flat distribution in M_{ee} . All MC productions, including all other ϕ decays, take into account changes in DAΦNE operation and background conditions on a run-by-run basis. Data-MC corrections for cluster energies and tracking efficiency, evaluated with radiative Bhabha events and $\phi \rightarrow \rho\pi$ samples, respectively, have been applied.

Preselection cuts require: i) four tracks in a cylinder around the interaction point (IP) plus two photon candidates; ii) best $\pi^+\pi^-\gamma\gamma$ match to the η mass using the pion hypothesis for tracks; iii) other two tracks assigned to e^+e^- ; iv) loose cuts on η and π^0 invariant masses ($495 < M_{\pi^+\pi^-\gamma\gamma} < 600$ MeV, $70 < M_{\gamma\gamma} < 200$ MeV). These simple cuts allow to clearly see the peak due to $\phi \rightarrow \eta e^+e^-$ events in the distribution of the recoil mass to the e^+e^- pair, $M_{\text{recoil}}(ee)$ (see fig. 1, left). A cut $535 < M_{\text{recoil}}(ee) < 560$ MeV is then applied.

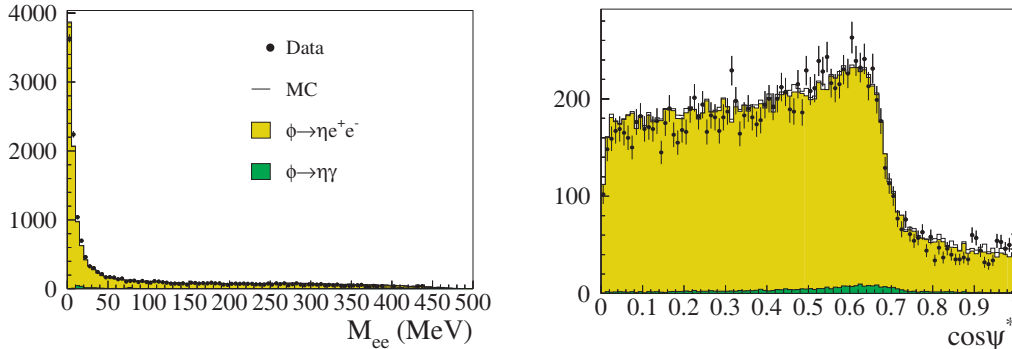


Fig. 2. – Invariant mass of the e^+e^- pair (left) and $\cos\psi^*$ distribution (right) for $\phi \rightarrow \eta e^+e^-$, $\eta \rightarrow \pi^+\pi^-\pi^0$ events.

A residual background contamination, due to $\phi \rightarrow \eta\gamma$ events with photon conversion on beam pipe (BP) or drift chamber walls (DCW), is rejected by tracing back the tracks of the two e^+ , e^- candidates and reconstructing their invariant mass (M_{ee}) and distance (D_{ee}) at the BP/DCW surfaces. As both quantities are small in case of photon conversions, $\phi \rightarrow \eta\gamma$ background is removed by rejecting events with: $M_{ee}(BP) < 10$ MeV and $D_{ee}(BP) < 2$ cm, $M_{ee}(DCW) < 80$ MeV and $D_{ee}(DCW) < 10$ cm. A further relevant background, originated by $\phi \rightarrow K\bar{K}$ and wrongly reconstructed $\phi \rightarrow \pi^+\pi^-\pi^0$ decays surviving analysis cuts, have more than two charged pions in the final state and are suppressed using time-of-flight (ToF) to the calorimeter. When an energy cluster is connected to a track, the arrival time to the calorimeter is evaluated both using the calorimeter timing (T_{cluster}) and the track trajectory ($T_{\text{track}} = L_{\text{track}}/\beta c$). The $\Delta T = T_{\text{track}} - T_{\text{cluster}}$ variable is then evaluated in both electron (ΔT_e) and pion (ΔT_π) hypotheses. Events with an e^+ , e^- candidate outside a 3σ 's window on the ΔT_e variables are rejected. In fig. 1, right, the M_{ee} distribution evaluated at different steps of the analysis is shown. The peaks at ~ 30 MeV and ~ 80 MeV are due to photon conversions on BP and DCW, respectively. The ToF cut reduces the tail at high M_{ee} values while the conversion cut removes events in the low invariant mass region. The analysis efficiency as a function of M_{ee} ranges between 10% and 20%, increasing for high M_{ee} values.

In fig. 2 the comparison between data and Monte Carlo events for M_{ee} and $\cos\psi^*$ distributions is shown. The second variable is the angle between the η and the e^+ in the e^+e^- rest frame. About 14000 $\phi \rightarrow \eta e^+e^-$, $\eta \rightarrow \pi^+\pi^-\pi^0$ candidates are present in the analyzed data set, with a negligible residual background contamination. As an accurate description of the background is crucial for the search of the U boson, its shape is extracted directly from our data. A fit is performed to the M_{ee} distribution, after applying a bin-by-bin subtraction of the $\phi \rightarrow \eta\gamma$ background and efficiency correction. The parametrization of the fitting function has been taken from ref. [37]:

$$(2) \quad \frac{d\Gamma(\phi \rightarrow \eta e^+e^-)}{dq^2} = \frac{\alpha}{3\pi} \frac{|F_{\phi\eta}(q^2)|^2}{q^2} \sqrt{1 - \frac{4m^2}{q^2}} \left(1 + \frac{2m^2}{q^2}\right) \lambda^{3/2}(m_\phi^2, m_\eta^2, m_U^2)$$

with $q = M_{ee}$ and the transition form factor described by $F_{\phi\eta}(q^2) = 1/(1 - q^2/\Lambda^2)$. Free parameters of the fit are Λ and an overall normalization factor. A good description of

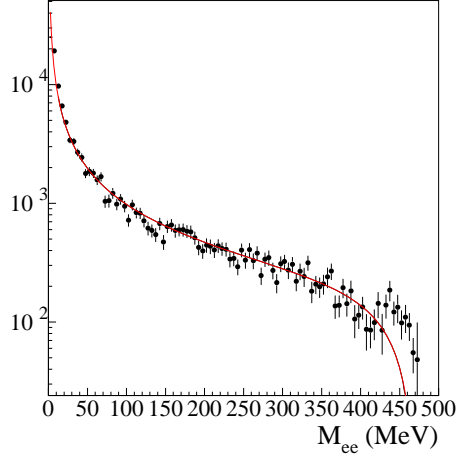


Fig. 3. – Fit to the M_{ee} spectrum for the Dalitz decays $\phi \rightarrow \eta e^+ e^-$, using the $\eta \rightarrow \pi^+ \pi^- \pi^0$ final state.

the M_{ee} shape is obtained, except at the high end of the spectrum (see fig. 3), where a residual background contamination from multi-pion events is still present.

As mentioned before, the $\phi \rightarrow \eta U$ MC signal has been produced according to ref. [22], with a flat distribution of the U boson invariant mass. Events are then divided in sub-samples of 1 MeV width. For each M_{ee} value, signal hypothesis has been excluded at 90% CL using the CL_S technique [38]. For the $\phi \rightarrow \eta U$ signal, the opening of the $U \rightarrow \mu^+ \mu^-$ threshold has been included, in the hypothesis that the U boson decays only to lepton pairs and assuming equal coupling to $e^+ e^-$ and $\mu^+ \mu^-$. The expected shape for the irreducible background $\phi \rightarrow \eta e^+ e^-$ is obtained from our fit to the M_{ee} distribution, taking also into account the error on number of background events as a function of M_{ee} . In fig. 4 the exclusion plot on $\alpha'/\alpha = \epsilon^2$ variable is compared with existing limits from the muon anomalous magnetic moment a_μ [39] and from recent measurements of the MAMI/A1 [40] and APEX [41] experiments. The gray line is where the U boson parameters should lay to account for the observed discrepancy between measured and calculated a_μ values. Our result greatly improves existing limits in a wide mass range, resulting in an upper limit on the α'/α parameter of $\leq 2 \times 10^{-5}$ at 90% CL for $50 < M_U < 420$ MeV.

3.2. The $\eta \rightarrow \pi^0 \pi^0 \pi^0$, $\eta \rightarrow \gamma \gamma$ final states. – Other two analyses devoted to the search of the $\phi \rightarrow \eta U$, $U \rightarrow e^+ e^-$, decay are in progress, using fully neutral η decay channels.

The analysis strategy for the $\eta \rightarrow \pi^0 \pi^0 \pi^0$ decay is similar to the previous one. After preselection cuts based on event topology, the background is reduced to negligible levels by cutting on the $e^+ e^-$ recoil mass, ToF variables and rejecting events due to conversions. The preliminary di-lepton invariant mass using 1.7 fb^{-1} is shown in fig. 5, left. Evaluation of the exclusion plot is in progress.

For the $\eta \rightarrow \gamma \gamma$ final state, the most severe background is generated by double radiative Bhabha scattering events and it is strongly reduced by cutting on the opening angle between the charged tracks and the photons. Residual non-Bhabha background is rejected by using further electron identification, based on the E/p ratio for the $e^+ e^-$

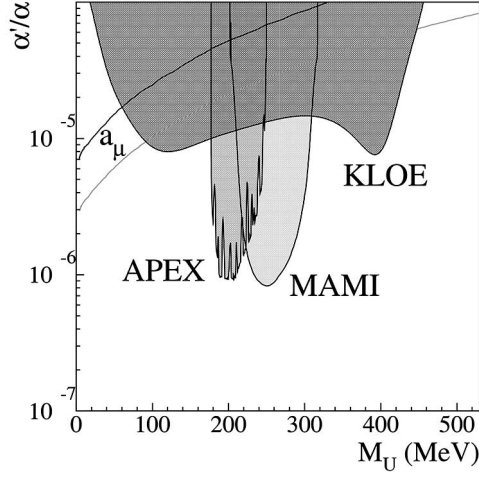


Fig. 4. – Exclusion plot at 90% CL for the parameter $\alpha'/\alpha = \epsilon^2$, compared with existing limits in our region of interest.

candidates. The resulting background reduction is still not enough for the search of $\phi \rightarrow \eta U$ events. The M_{ee} spectrum obtained with 1.7 fb^{-1} (fig. 5, right) shows a clear evidence of $\phi \rightarrow \eta e^+e^-$ Dalitz decays at low values and a residual background contamination at high M_{ee} due to Bhabha events. Work is in progress to further improve the signal-to-background ratio.

4. – The Higgs'-strahlung channel

The feasibility of the search for the process $e^+e^- \rightarrow Uh'$ has been done considering the $m_{h'} < m_U$ case. At DAΦNE energies, for $\epsilon \sim 10^{-3}$, a production cross-section of $\approx 20 \text{ fb}$ is expected and the h' has $\tau_{h'} > 10 \mu\text{s}$, escaping the detection. The signature is therefore a lepton pair from the U boson plus missing energy.

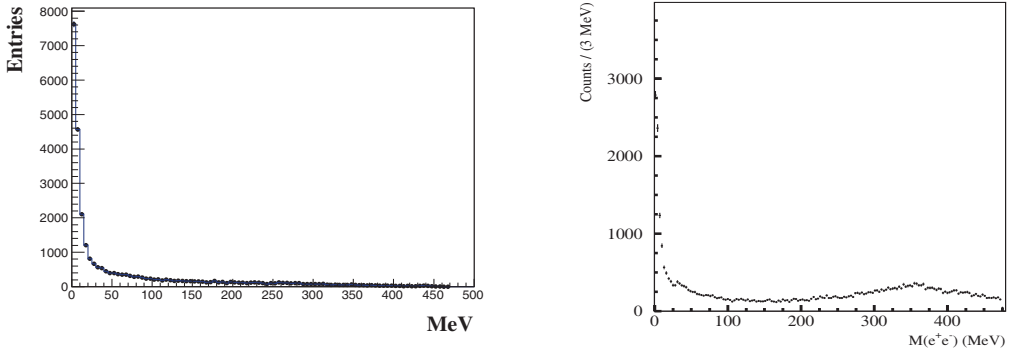


Fig. 5. – Invariant mass of the e^+e^- pair for $\eta \rightarrow \pi^0\pi^0\pi^0$ (left) and $\eta \rightarrow \gamma\gamma$ (right) channels.

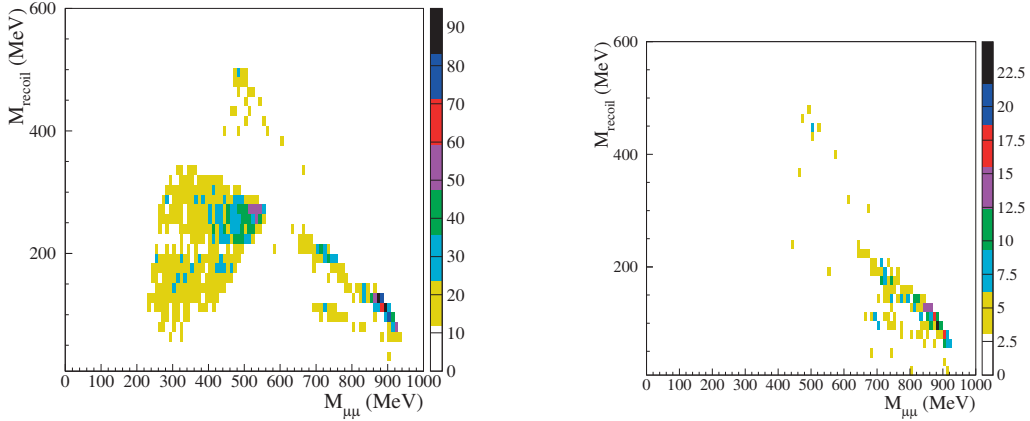


Fig. 6. – Search for $e^+e^- \rightarrow h'U$, $U \rightarrow \mu^+\mu^-$, $h' \rightarrow$ “invisible” events: recoil mass to the $\mu^+\mu^-$ pair as a function of the di-muon invariant mass for data taken at the ϕ mass (left) and at $\sqrt{s} = 1$ GeV (right).

The selection strategy has been optimized using Monte Carlo events. The signal has been generated according to ref. [20] in a discrete set of mass values in the range $m_U \leq 900$ MeV, $m_{h'} \leq 400$ MeV. The $U \rightarrow e^+e^-$ events are not selected by any official KLOE event classification (ECL) algorithms, which divide the events on the basis of topological information and provide reconstructed data to be used for different analyses. On the contrary, ECL is fully efficient for $U \rightarrow \mu^+\mu^-$ events when $m_{h'} < 300$ MeV. We therefore considered the $\mu^+\mu^-$ final state only.

Muons are identified and separated from electrons and pions using a neural network algorithm based on energy depositions along the shower depth in the calorimeter and E/p , β variables. The other relevant cuts to reduce background contamination are: i) missing momentum direction in the barrel calorimeter; ii) a tight cut on vertex-IP distance and iii) no clusters in the calorimeter, with the exception of the two associated to tracks. The residual background contamination is due to $e^+e^- \rightarrow \pi^+\pi^-\gamma/\mu^-\mu^-\gamma$ continuum events with an undetected photon, and to $\phi \rightarrow K^+K^- \rightarrow \mu + \mu^-\nu\bar{\nu}$ with early decaying kaons.

In fig. 6, left the distribution of the recoil mass to the $\mu^+\mu^-$ pair (M_{recoil}) as a function of the di-muon invariant mass obtained with 1.65 fb^{-1} is reported. M_{recoil} is evaluated using the center-of-mass energy of each run measured with Bhabha scattering events and the momenta of the muons. Continuum background, which can be further reduced tuning the π/μ identification algorithm, is concentrated in the band at $M_{\mu^+\mu^-} > 700$ MeV. The $\phi \rightarrow K^+K^-$ channel covers a wider region of the plane ($M_{\mu^+\mu^-} < 600$ MeV, $M_{\text{recoil}} < 300$ MeV). This background, having only two muons in the final state and missing energy due to neutrinos, has the same signature of the signal. The efficiency for $e^+e^- \rightarrow Uh'$ events is 15–40%, depending on m_U , $m_{h'}$ masses. Taking into account the total integrated luminosity, a signal would show up as a sharp peak with ≤ 10 events in the $M_{\text{recoil}}-M_{\mu\mu}$ plane for $\epsilon \sim 10^{-3}$.

Being the $\phi \rightarrow K^+K^-$ background a nasty background source, we repeated the analysis using the off-peak sample, 0.2 fb^{-1} taken at a center-of-mass energy of 1 GeV. As can be seen in fig. 6, right, the contribution from resonant background is not present anymore, providing a much cleaner sample for the search of $e^+e^- \rightarrow Uh'$ candidates.

5. – Summary and perspectives for KLOE-2

The search for $\phi \rightarrow \eta U$ with $U \rightarrow e^+e^-$, $\eta \rightarrow \pi^+\pi^-\pi^0$, using 1.5fb^{-1} of KLOE data, results in an upper limit on the $\alpha'/\alpha = \epsilon^2$ parameter of $\leq 2 \times 10^{-5}$ at 90% CL for $50 < M_U < 420\text{MeV}$. The inclusion of the the $\eta \rightarrow \pi^0\pi^0\pi^0$ and $\eta \rightarrow \gamma\gamma$ channels, already under study, will cover 95% of the η decay channels. Due to larger branching ratio and analysis efficiency, an improvement of ≈ 2 on the upper limit is expected. With the new data sample expected at KLOE-2, this value can be further improved. An integrated luminosity 10fb^{-1} will provide another factor 2 improvement on the upper limit evaluation.

The search of the Higgs'-strahlung channel, $e^+e^- \rightarrow Uh'$ with $U \rightarrow \mu^+\mu^-$ plus missing energy, is limited by a non-negligible $\phi \rightarrow K^+K^-$ background in a wide region of the $M_{\mu^+\mu^-}$, M_{recoil} plane. Work is in progress to reduce this contribution on the KLOE data sample. At KLOE-2, the improvement on the vertex resolution, achievable with the insertion of the inner tracker, will provide a higher rejection factor. The feasibility of a high statistics run at 1 GeV, where the resonant background contribution is naturally reduced, is also under discussion.

* * *

I would like to warmly thank the organizers for their invitation and for the kind hospitality. This work was supported in part by the EU Integrated Infrastructure Initiative HadronPhysics Project under contract number RII3-CT-2004-506078; by the European Commission under the 7th Framework Programme through the ‘‘Research Infrastructures’’ action of the ‘‘Capacities’’ Programme, Call: FP7-INFRASTRUCTURES-2008-1, Grant Agreement N. 227431; by the Polish Ministry of Science and Higher Education through the Grant No. 0469/B/H03/2009/37.

REFERENCES

- [1] JEAN P. *et al.*, *Astron. Astrophys.*, **407** (2003) L55.
- [2] ADRIANI O. *et al.*, *Nature*, **458** (2009) 607.
- [3] CHANG J. *et al.*, *Nature*, **456** (2008) 362.
- [4] ABDO A. A. *et al.*, *Phys. Rev. Lett.*, **102** (2009) 181101.
- [5] AHARONIAN F. *et al.*, *Phys. Rev. Lett.*, **101** (2008) 261104.
- [6] AHARONIAN F. *et al.*, *Astron. Astrophys.*, **508** (2009) 561.
- [7] BERNABEI R. *et al.*, *Int. J. Mod. Phys. D*, **13** (2004) 2127.
- [8] BERNABEI R. *et al.*, *Eur. Phys. J. C*, **56** (2008) 333.
- [9] AALSETH C. E. *et al.*, *Phys. Rev. Lett.*, **107** (2011) 141301.
- [10] POSPELOV M., RITZ A. and VOLOSHIN M. B., *Phys. Lett. B*, **662** (2008) 53.
- [11] ARKANI-HAMED N., FINKBEINER D. P., SLATYER T. R. and WEINER N., *Phys. Rev. D*, **79** (2009) 015014.
- [12] ALVES D. S. M., BEHBAHANI S. R., SCHUSTER P. and WACKER J. G., *Phys. Lett. B*, **692** (2010) 323.
- [13] POSPELOV M. and RITZ A., *Phys. Lett. B*, **671** (2009) 391.
- [14] HISANO J., MATSUMOTO S. and NOJIRI M. M., *Phys. Rev. Lett.*, **92** (2004) 031303.
- [15] CIRELLI M., KADASTIK M., RAIDAL M. and STRUMIA A., *Nucl. Phys. B*, **813** (2009) 1.
- [16] MARCH-RUSSELL J., WEST S. M., CUMBERBATCH D. and HOOPER D., *JHEP*, **07** (2008) 058.
- [17] CHOLIS I., DOBLER G., FINKBEINER D. P., GOODENOUGH L. and WEINER N., *Phys. Rev. D*, **80** (2009) 123518.
- [18] CHOLIS I., FINKBEINER D. P., GOODENOUGH L. and WEINER N., *JCAP*, **12** (2009) 007.

- [19] ARKANI-HAMED N. and WEINER N., *JHEP*, **12** (2008) 104.
- [20] BATELL B., POSPELOV M. and RITZ A., *Phys. Rev. D*, **79** (2009) 115008.
- [21] ESSIG R., SCHUSTER P. and TORO N., *Phys. Rev. D*, **80** (2009) 015003.
- [22] REECE M. and WANG L. T., *JHEP*, **07** (2009) 051.
- [23] BORODATCHENKOVA N., CHOUDHURY D. and DREES M., *Phys. Rev. Lett.*, **96** (2006) 141802.
- [24] YIN P. F., LIU J. and ZHU S. H., *Phys. Lett. B*, **679** (2009) 362.
- [25] BJORKEN J. D., ESSIG R., SCHUSTER P. and TORO N., *Phys. Rev. D*, **80** (2009) 075018.
- [26] BATELL B., POSPELOV M. and RITZ A., *Phys. Rev. D*, **80** (2009) 095024.
- [27] ESSIG R., SCHUSTER P., TORO N. and WOJTSEKHOWSKI B., *JHEP*, **02** (2011) 009.
- [28] FREYTSIS M., OVANESYAN G. and THALER J., *JHEP*, **01** (2010) 111.
- [29] FAYET P., *Phys. Lett. B*, **95** (1980) 285; **187** (1981) 184.
- [30] BOEHM C. and FAYET P., *Nucl. Phys. B*, **683** (2004) 219.
- [31] FAYET P., *Phys. Rev. D*, **70** (2004) 023514.
- [32] BOSSI F. *et al.*, *Riv. Nuovo Cimento*, **031** (2008) 531.
- [33] MILARDI C. *et al.*, *ICFA Beam Dyn. Newslett.*, **48** (2009) 23.
- [34] AMELINO-CAMELIA G. *et al.*, *Eur. Phys. J. C*, **68** (2010) 619.
- [35] ACHASOV M. N. *et al.*, *Phys. Lett. B*, **504** (2001) 275.
- [36] AKHMETSHIN R. R. *et al.*, *Phys. Lett. B*, **501** (2001) 191.
- [37] LANDSBERG L. G., *Phys. Rep.*, **128** (1985) 301.
- [38] JUNK T., *Nucl. Instrum. Methods A*, **434** (1999) 435.
- [39] POSPELOV M., *Phys. Rev. D*, **80** (2009) 095002.
- [40] MERKEL H. *et al.*, *Phys. Rev. Lett.*, **106** (2011) 251802.
- [41] ABRAHAMYAN S. *et al.*, *Phys. Rev. Lett.*, **107** (2011) 191804.